Interface Asymmetry Induced by Symmetric Electrodes on Metal–Al:TiO$_x$–Metal Structures

Loukas Michalas, Maria Trapatseli, Spyros Stathopoulos, Simone Cortese, Ali Khiat, and Themistoklis Prodromakis, *Senior Member, IEEE*

***Abstract*—Emerging memory technologies have sparked great interest in studying a variety of materials that can be employed in metal–insulator–metal topologies to support resistive switching. While the majority of reports focus on identifying appropriate materials that can be used as active core layers, the selection of electrodes also impacts the performance of such memory devices. Here, both the top and the bottom interfaces of symmetric Metal–Al:TiO$_x$–Metal structures have been investigated by the analysis of their current versus voltage characteristics in the temperature range of 300–350 K. Three different metals were utilized as electrodes, Nb, Au, and Pt, for covering a wide range of work function and electronegativity values. Despite their symmetric structure, the devices were found to exhibit asymmetric performance with respect to the applied bias polarity. Clear signature plots indicating thermionic emission over the interface Schottky barriers have been obtained. The asymmetry between the top and the bottom interfaces was further evaluated by the values of the potential barrier heights and by the barrier lowering factors, both calculated from the experimental data. This study highlights the importance of the interface effects and proves that in addition to film doping, proper (top/bottom) metal selection, and interface engineering should also be exploited for developing thin film metal oxide based devices with tailored electrical characteristics.**

***Index Terms*—Contacts, doping, interface, metal oxide, TiO$_2$, RRAM.**

I. Introduction

THIN metal oxide (MO) films have attracted great attention over the last decade, mainly due to their promising exploitation in a variety of applications, including memristive devices/Resistive Random Access Memories (RRAMs) [1], [2], neuromorphic systems [3], [4], semiconductor devices [5] and sensing [6]. A key parameter for their unique ensemble of properties is their oxygen content [7], [8] that is mainly determined by the film deposition conditions [9].

Manuscript received July 27, 2017; revised November 10, 2017; accepted November 15, 2017. Date of publication December 19, 2017; date of current version September 6, 2018. This work was supported by the EPSRC Grant EP/K017829/1. All data supporting this study are openly available from the University of Southampton repository at: http://doi.org/10.5258/SOTON/D0307. The review of this paper was arranged by the MEMRISYS 2017 Guest Editors.
(Corresponding author: Loukas Michalas.)

The authors are with the Nanoelectronics and Nanotechnology Research Group, Department of Electronics and Computer Science, University of Southampton, Southampton SO17 1BJ, U.K. (e-mail: l.michalas@soton.ac.uk; mt3c13@soton.ac.uk; S.Stathopoulos@soton.ac.uk; sc2v14@soton.ac.uk; A.Khiat@soton.ac.uk; t.prodromakis@soton.ac.uk).

Color versions of one or more of the figures in this paper are available online at http://ieeexplore.ieee.org.

Digital Object Identifier 10.1109/TNANO.2017.2777698

A late trend towards the development of MO films with desirable electrical characteristics is the introduction of appropriate dopants that could affect the formation energy for the oxygen vacancies and thus allow tailoring the MO film electrical properties [10]. As an example, the introduction of Al in TiO$_2$, that is one of the most celebrated MO, revealed improved switching characteristics in RRAMs [11], while it is theoretically predicted that Al could also act as "acceptor" type dopant enabling p-type conductivity [12].

Apart from the MO device active layer however, the electrode materials have also an important role on the device performance. The importance of the metal/MO interfacial effects is further enhanced by the downscaling trend along with the implementation of thin MO films on state of the art devices.

Their complete understanding is therefore of vital importance for the development of MO based semiconductor devices [13], [14]. Moreover, it has been reported that Schottky type contact is essential on TiO$_2$ to enable resistive switching [15], making the study of the interface effects of particular interest also for memristor based application. In turn, the properties of Metal/TiO$_2$ interfaces are intensively studied by several groups over the recent years [16]–[22].

Regarding the metal/semiconductor interface, typically a Schottky barrier is formed. The barrier height is given by the difference between the metal work function and semiconductor electron affinity [23], thus allowing its modifications by the proper metal electrode selection. In contrast to the conventional semiconducting materials, this well-defined theory cannot directly be applied on Metal/TiO$_2$ interfaces. Experimental results demonstrated that this is not a traditional Schottky barrier and rather than the metal work function, it is the metal electronegativity [16], the interface reaction [18], [19], or even the design and/or fabrication details [20]–[22] that could determine the interface properties, although further investigations are still required towards thorough clarification. A common approach on the aforementioned studies is the implementation of distinct metal contacts formed at the top of the TiO$_2$ films and are benchmarked via the room temperature assessment of their current-voltage characteristic.

Considering these aspects, the paper aims to present a quantitative experimental study on the characteristics of both the top and the bottom electrode interfaces on Metal-Al:TiO$_x$-Metal structures, linking the timely research fields of the film doping and interface characterization. For this, symmetric devices, depicted in Fig. 1, were fabricated using three different electrode

This work is licensed under a Creative Commons Attribution 3.0 License. For more information, see http://creativecommons.org/licenses/by/3.0/

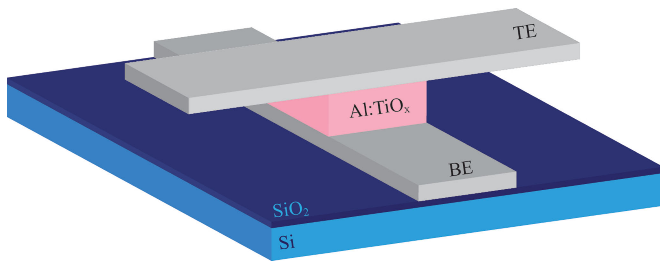

Fig. 1. Schematic of the symmetric Metal-Al:TiO_x-Metal structures. Nb, Au and Pt have been chosen as both top (TE) and bottom (BE) electrodes.

TABLE I
COMMONLY ADOPTED VALUES FOR THE METALS WORK FUNCTION AND ELECTRONEGATIVITY [16]

Metal Electrode	Work Function (eV)	Electronegativity
Nb	4.3	1.6
Au	5.1	2.4
Pt	5.65	2.2

materials, namely: Nb (Niobium), Au (Gold) and Pt (Platinum). These electrodes have been chosen in order to cover a wide range of work function and electronegativity values, as denoted in Table I, which constitutes two quantitative parameters that is expected [16], [23] to determine the interface barriers.

Moreover, bearing in mind that there are more than one conduction mechanisms across the wide band gap materials that exhibit exponential dependence on the applied electric field [23], all electrical characterization were carried out in the temperature range of 300 K to 350 K. This way clear field and temperature dependent signature plots of the dominant conduction mechanism were obtained, allowing also quantitative interpretation of the experimental data.

II. Experimental

The tested devices were fabricated on separate 6 inch Si wafers having a 200 nm thick SiO_2 layer that was grown by dry oxidation. The electrodes and the active layers were patterned by optical lithography. Bottom (on top of 5 nm thick Ti adhesion layer) and top 15 nm thick Au and Pt electrodes were deposited via electron beam evaporation, while the identical Nb ones were deposited by magnetron sputtering. The Al:TiO_x films were deposited by reactive co-sputtering (Helios XP, Leybold optics) using simultaneously a Ti (operated at 2 kW) and an Al (operated at 50 W) targets in oxygen plasma environment, following the recipe described in details in [11]. Films with thickness of 45 nm were finally obtained as evaluated by spectroscopic ellipsometry (Woolham M-2000) using the Lorentz model.

X-ray Photoelectron Spectroscopy (XPS) characterization was utilized to evaluate the Al content in the Al:TiO_x films. The spectra was recorded by means of a Thermo Scientific Theta Probe angle resolved photoelectron spectrometer system, having a X-ray source corresponds to hv = 1486.6 eV. After appropriate post process of the recorded spectra, Al concentration was found to be 4% at., taking into account in the quantification only the cations of Ti and Al [11].

The current vs voltage (I–V) characteristics were obtained on $30 \times 30\ \mu m^2$ standalone RRAM like stacks using our in-house memristor characterization platform [24], ArC ONE, along with a probe card that allowed multiple devices characterization. The voltage sweeping were carried out in staircase mode towards positive biases, while both the positive and negative polarities were always applied to the top electrode (TE) with respect to the bottom electrode (BE) that was continuously kept at ground potential via the instrumentation. The experiments were performed on a Cascade SUMMIT 12000B semi-automatic probe station that incorporates a thermal chuck which can be externally biased and whose temperature can be controlled by an ESPEC ETC-200L unit. Measurements were performed by keeping the chuck grounded and at various temperatures in the range of 300 K to 350 K, with a 10 K step.

III. Results and Discussion

The typically acquired temperature-dependent current voltage characteristics of our device prototypes having Nb, Au and Pt electrodes are presented in Fig. 2(a)–(c) respectively. Devices with Nb electrodes were found to exhibit a soft breakdown when the applied electric field reaches intensities in the order of 400 KV/cm (1.5 V–2 V). Therefore, in this case the measurements were limited to low applied biases (±1 V) for ensuring reliable operation across the studied temperature range (Fig. 2(a)). In contrast, the devices with Au and Pt electrodes were possible to test with field intensities in excess of 1 MV/cm. For all cases, our results present an asymmetric electrical behavior with respect to the applied bias polarity. In order to confirm that this asymmetry does not arise by any substrate induced effect (the substrate Metal-Oxide-Semiconductor (MOS) formed capacitor has been reported to affect Capacitance-Voltage (C–V) measurements [25] along with the interface states that induce losses on RF performance [26]), preliminary measurements performed with the substrate both floating and grounded revealed absolutely any differences. This is because in our case we perform DC current-voltage (I–V) measurements on a vertical stack with respect to a grounded bottom electrode formed atop the high quality thermal oxide. The configuration offers adequate isolation to any substrate induced leakage current. This can also be experimentally verified in Fig. 2(c) where negligible current flow is measured up to applied voltages exciding 2.5 V. Therefore the obtained asymmetry is attributed purely to interface controlled transport mechanism and in particular denoting deviation in the properties of the two interfaces despite their nominal symmetric structure.

Following from this result and taking into account the n-type character of the Al:TiO_x film (although Al is expected to act as p-type dopant [12], p-type character was not obtained in our films), the devices should equivalently be modeled as presented in Fig. 3.

For the latter configuration, when a positive bias is applied to the TE, the TE/Al:TiO_x contact will be forward biased whilst

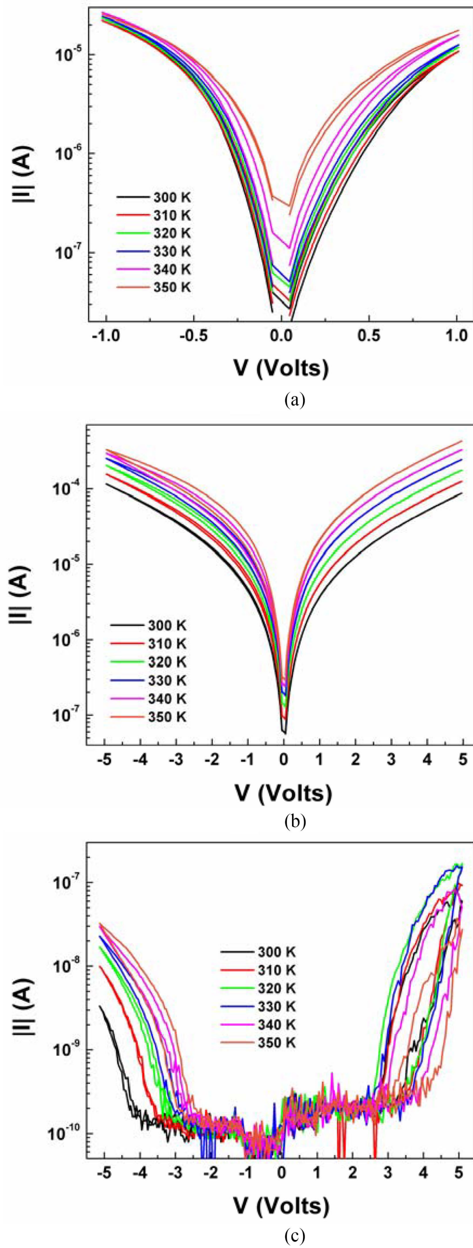

Fig. 2. Current vs voltage (I–V) characteristics recorded in the temperature range of 300 K to 350 K on devices having (a) Nb, (b) Au and (c) Pt electrodes.

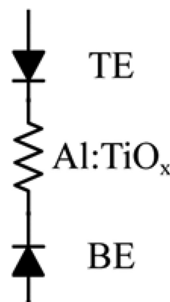

Fig. 3. Based on the obtained asymmetry in their performance the devices can equivalently be represented by a series combination of electronic elements.

the Al:TiO$_x$/BE reversed biased and vice-versa. In this case, the current flow across the structure is practically determined by the reversed biased contact (the most resistive element), thus by the bottom one for the positive biases and by the top one for the negative ones respectively.

Following this perspective, the experimental results have been further analyzed in terms of the thermionic emission over a constant Schottky barrier given by [23], [27]

$$I = AT^2 e^{-\frac{\Phi_{B0}-a\sqrt{V}}{KT}} \tag{1}$$

where K is the Boltzmann constant, T is the absolute temperature, Φ_{B0} is the zero bias potential barrier height at Metal/MO interface and A = (Area × A*), with A* being the Richardson constant and "α" the barrier lowering factor.

In order to confirm thermionic emission as the responsible mechanism dominating the transport, the experimental data for any specific electric field (V), should exhibit a linear behavior on a $\ln(I/T^2)$ vs $1000/T$ plot. In such a plot, the slope yields to an activation energy, E, (2) that corresponds to the apparent potential barrier Φ_{APP} under this specific applied field intensity (equivalently V).

$$E = \Phi_{APP} = \Phi_{B0} - a\sqrt{V} \tag{2}$$

Moreover, this activation energy/apparent barrier should decrease with increasing the applied bias V. Further to this, by plotting the experimentally obtained apparent barrier values, in a Φ_{APP} vs $\sqrt{V}$ plot, it should yield a straight line (2). The analysis of the experimental data in the above perspective is presented in Fig. 4.

Clear signature plots obtained for all the contacts with the exception of the Pt BE. In this case the I–V form (Fig. 2(c)) denotes notable contribution from ions motions that possibly modify the interface barrier during the I–V acquisition and thus the analysis with respect to a mechanism corresponds to electronic transport over a constant barrier would not be valid. Similarly some specific high temperature I–Vs in the other two cases, e.g., 340 K and 350 K for Nb contacts (Fig. 2(a)), deviate from the expected behavior. This deviation is attributed to the onset of a transition regime towards another higher temperature dominant mechanism.

The well-defined signature plots presented in Fig. 4 constitutes strong experimental evidence supporting the thermionic emission over the TE/BE-interface Schottky barrier (1) as the mechanism dominating the transport. In the presence of these clear signature plots, Fig. 4(f) can be further assessed yielding additional quantitative information. The slope of this plot corresponds to the barrier lowering factor "α", a parameter that is strongly interface dependent, while the intercept extrapolated to V = 0 V, provides the zero bias potential barrier (Φ_{B0}) formed at the interface (2). Only in cases where both signatures are satisfied, the quantitative analysis can be considered. As a counterexample it is worth pointing out the low field performance in case of Au contacts.

In this case although clear signatures obtained in Fig. 4(c) and (d), it reveals that the apparent barrier tends to saturate for biases below 1 V (Fig. 4(f)). Therefore we may

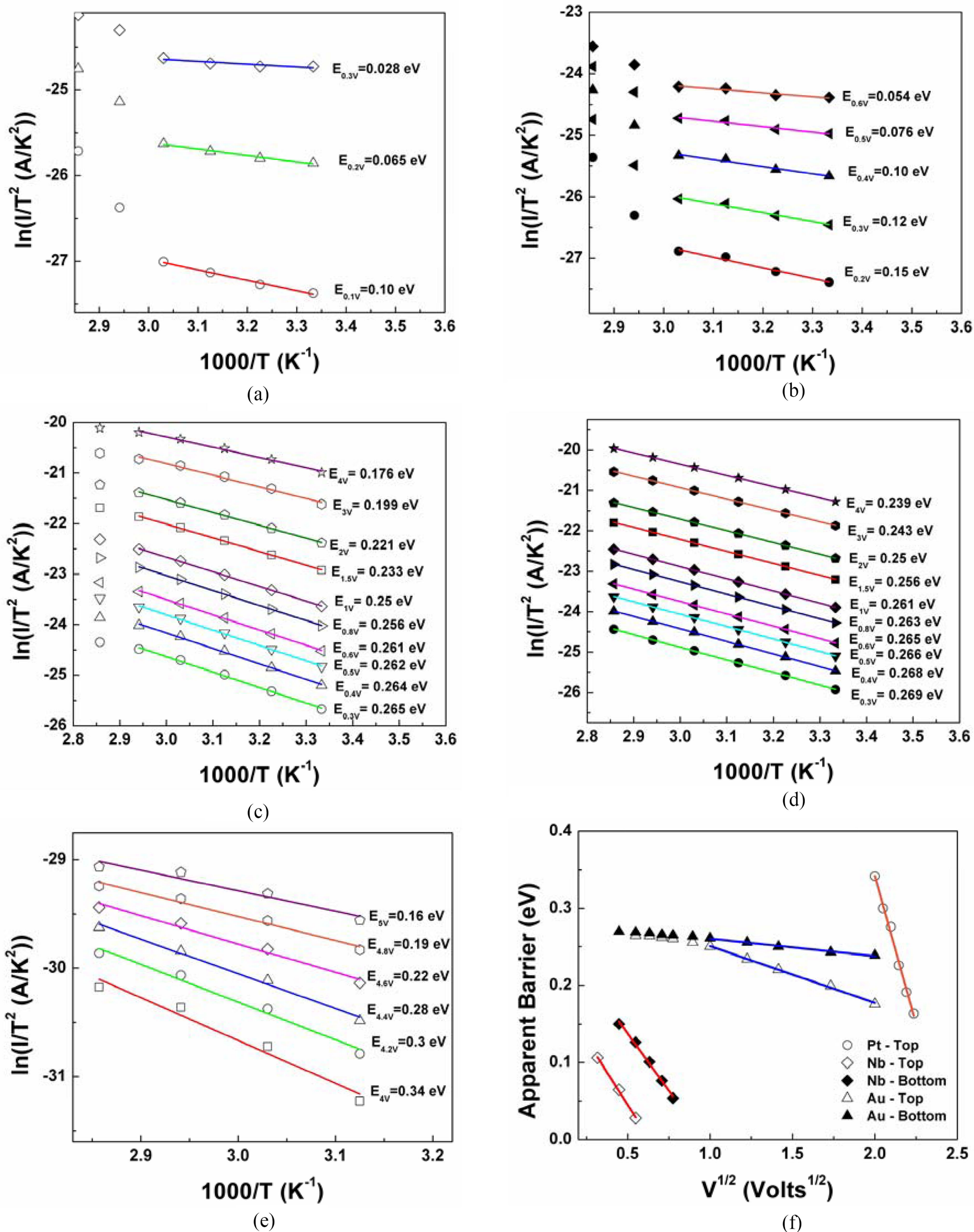

Fig. 4. Signature plots confirming thermionic emission as the major mechanism for (a) Nb top and (b) bottom electrode, for (c) Au top and (d) bottom electrode and for (e) Pt top. An additional confirmation for all cases is offered by the linear relation in (f), yielding also to quantitative results (Table II).

TABLE II
BARRIER LOWERING FACTOR ("α") AND ZERO BIAS POTENTIAL BARRIERS (Φ_{B0}), OBTAINED FROM THE ANALYSIS OF THE SIGNATURE PLOTS

Metal Electrode	Interface	Φ_{B0} (eV)	α (eV$^{1/2}$)
Nb	Top	0.21	0.337
	Bottom	0.28	0.296
Au	Top	0.33	0.074
	Bottom	0.29	0.023
Pt	Top	1.87	0.768

conclude that thermionic emission cannot be considered as the dominant mechanism in this regime (most probably more than one mechanism are determining the transport) and therefore these results are not included in the estimation of the Schottky barrier. Following this perspective the corresponding results are summarized in Table II and clearly verify the experimentally obtained asymmetry.

In contrast to the Schottky theory for the conventional metal-semiconductor barriers, where their height is directly proportional to the metal work function [23], a different condition has been experimentally observed in the case of top metal-"undoped" TiO_2 contacts formed on devices having an ohmic bottom contact. Room temperature studies focusing on either the rectification ratio at read-out voltage of ±1 V, or on room temperature calculations of the barrier height, revealed that it is the metal electronegativity rather than the work function that plays a dominant role on the carrier transport [16]. Similarly and by assessing the room temperature resistance of the stacks measured at ±1 V, it was confirmed that it is not the work function that dominates the contact but mainly the formation free energy of the metal electrode oxides that determines the measured resistance [18]. Both studies discussed their findings by attributing an important role to the oxygen vacancies and interface states.

In our case (Al:TiO_x), the quantitative results obtained by leveraging both field and temperature dependence of the I–V characteristics and through the above discussed corresponding signature plots, did not reveal any straightforward correlation to the metal work function or to the electronegativity/formation free energy. Moreover the asymmetry found in both the potential barriers height (Φ_{B0}) and the barrier lowering factors (α), between the symmetric top and bottom contacts (Table II), clearly indicate the dominant role of the interface effects on the device performance. An additional parameter that should be considered is the Al doping that is expected to differentiate the film microstructure and energy vacancies formation with respect to the "undoped" TiO_2 films.

Although further studies are still required in order to fully clarify the physics of metal/MO contacts, a possible origin of the obtained asymmetry even in our symmetric structures, could be the differences during the formation of the two interfaces. From the electrical characterization perspective this correspond to different amount and distribution of interface states. Interface states are affecting the electrical characteristics of semiconductor devices by trapping charges and thus by determining the surface potential and the Fermi level position. In particular for Metal/TiO_2 top contacts, partial pinning has been reported [16]. The asymmetry is expected in deposited materials as the oxide film is growing on top of a foreign material (bottom electrode). This could be even more complicated when the deposited atoms interact with the electrode metals. Moreover the film should effectively adapt any imperfection such as the surface roughness of the bottom electrode. It is worth in particular mentioning the roughness of the bottom electrode as a parameter that has been found to have a major role on the film microstructure and thus to critically determine the electrical behavior of e.g., silicon-oxide ReRAMs [28], [29]. The important role of the bottom electrode/interface in addition to the top one is also depicted in our results through two more I–V curves features. The Al:TiO_x films grown on the Nb bottom electrodes were found to undergo a soft irreversible breakdown under electric field intensity in the order of 400 KV/cm (Fig. 2(a)). In contrast, the films grown on Au (Fig. 2(b)) and Pt (Fig. 2(c)), following the same deposition recipe, can withstand electric fields exceeding 1 MV/cm. Moreover, the films on Pt bottom contact exhibit strong ionic characteristics, denoting the presence of movable ions, while no such behavior obtained on devices having Au electrodes under the same electric fields.

On the contrary to the bottom interfaces, the upper material layers are deposited on the material itself and thus less interactions are expected. The top metal contact is therefore deposited on the already well-formed oxide material and it is the metal that has to adapt the film structure at this final fabrication step. In this case the fabrication details have been also reported to affect the contact properties [21].

These results strongly support that any metal contact should be assessed with respect to whether it will be used as top or bottom electrode. This choice could prove to be critical for the performance of metal-oxide based electronic devices.

Commonly Metal-TiO_2-Metal devices are implemented on RRAM applications. For this, electroforming is a necessary step for most technologies and the observed asymmetry could play a role both in terms of the electroforming efficiency (and/or polarity dependence) as well as the switching performance of RRAM devices. Regarding our Al:TiO_x films, (resistive switching effects on stacks with Pt contacts that have been reported in details in our previously published work [11]), those were found to exhibit asymmetric behavior even after the forming process as revealed by the post forming I–V characterization as well as by their analog switching behavior [11].

Another timely research field to incorporate the above result, is the design of forming free RRAM cells or of oxide based selectors. As an example, asymmetric performance has also been reported on symmetric Ni/TiO_2/Ni stacks [30]. The choice of the metal electrodes could define the symmetry/asymmetry in bipolar resistive switching or to be used to determine the optimum polarity and the magnitude of the Readout voltage in non-volatile RAMs.

Moreover, this is also of particular interest for designing more complicated structures such as the vertically integrated [31], 1 diode (1D) 1 switching resistor (1R) ones. In such 1D1R stacks, beyond the usual adoption of a Schottky type contact for the 1D part [32] (thus the need for assessing the Metal/Mo contact), the two elements (1D/1R) may be interconnected using a common electrode [31]. This common electrode will be then TE for the

lower part and the BE for the upper part of the structure and therefore has to be accordingly selected. Additionally, for applications beyond the memories, it is worth also mentioning the metal contacts at the source and the drain terminals of MO based Thin Film Transistors (TFTs), very recently reported to affect the device performance [33]. In the case of TFTs, the metal contacts could also be at the top or at the bottom of the active area (MO film) depending on the device structure (top or bottom gate) and on the preferred configuration (staggered or coplanar).

IV. Conclusion

In summary, both the top and the bottom interface characteristics of symmetric Metal-Al:TiO_x-Metal structures for three distinct electrode materials (Nb, Au, Pt) have been reported. Based on the acquired field and temperature dependent signature plots, thermionic emission over the Schottky barriers was identified as the dominant transport mechanism around room temperature. The top and bottom interfaces were found to exhibit asymmetric characteristics despite their symmetric structure. Our reported quantitative results suggest that any metal should be assessed with respect to whether it will be used as top or bottom electrode, highlighting the importance of the interface effects. Overall, this study demonstrates that in addition to the doping of the oxide film, proper top and bottom electrode selection and interface engineering should also be carefully considered when optimizing MO-based devices (RRAM, 1D1R, TFT) for attaining desirable performance.

References

[1] J. J. Yang, D. B. Strukov, and D. R. Stewart, "Memristive devices for computing," *Nature Nanotechnol.*, vol. 8, pp. 13–24, 2013.

[2] D. Ielmini, "Resistive switching memories based on metal oxides: Mechanisms reliability and scaling," *Semicond. Sci. Technol.*, vol. 31, 2016, Art. no. 063002.

[3] M. Prezioso, F. Merrikh-Bayat, B. D. Hoskins, G. C. Adams, K. K. Likharev, and D. B. Strukov, "Training and operation of an integrated neuromorphic network based on metal-oxide memristors," *Nature*, vol. 521, pp. 61–64, 2015.

[4] A. Serb, J. Bill, A. Khiat, R. Berdan, R. Legenstein, and T. Prodromakis, "Unsupervised learning in probabilistic neural networks with multi-state metal-oxide memristive synapses," *Nature Commun.*, vol. 7, 2016, Art. no. 12611.

[5] Z. Wang, P. K. Nayak, J. A. Caraveo-Frescas, and H. N. Alshareef, "Recent developments in p-type oxide semiconductor materials and devices," *Adv. Mater.*, vol. 28, pp. 3831–3892, 2016.

[6] G. F. Fine, L. M. Gavanagh, A. Afonja, and R. Binions, "Metal oxide semiconductor gas sensors in environmental monitoring," *Sensors*, vol. 10, pp. 5469–5502, 2010.

[7] Y. C. Bae, A. R. Lee, J. S. Kwak, H. Im, and J. P. Hong, "Dependence of resistive switching behaviors on oxygen content of Pt/TiO_{2-x}/Pt matrix," *Current Appl. Phys.*, vol. 11, pp. e66–e69, 2011.

[8] I. Salaoru, T. Prodromakis, A. Khiat, and C. Toumazou, "Resistive switching of oxygen enhanced TiO_2 thin film devices," *Appl. Phys. Lett.*, vol. 102, 2013, Art. no. 013506.

[9] V. C. Anitha, A. N. Benerjee, and S. W. Joo, "Recent developments in TiO_2 as n- and p- type transparent semiconductors: synthesis, modification, properties, and energy related applications," *J. Mater. Sci.*, vol. 50, pp. 7495–7536, 2015.

[10] H. Jiang and D. A. Stewart, "Using dopants to tune oxygen vacancy formation in transition metal oxide resistive memory," *ACS Appl. Mater. Interfaces*, vol. 9, pp. 16296–16304, 2017.

[11] M. Trapatseli, A. Khiat, S. Cortese, A. Serb, D. Carta, and T. Prodromakis, "Engineering the switching dynamics of TiO_x-based RRAM with Al doping," *J. Appl. Phys.*, vol. 120, 2016, Art. no. 025108.

[12] L. Zhao, S.-G. Park, B. Magyari-Kope, and Y. Nishi, "Dopant selection rules for desired electronic structure and vacancy formation characteristics of TiO_2 resistive memory," *Appl. Phys. Lett.*, vol. 102, 2013, Art. no. 083506.

[13] A. T. Iancu, M. Logar, J. Park, and F. B. Prinz, "Atomic layer deposition of undoped TiO_2 exhibiting p-type conductivity," *ACS Appl. Mater. Interfaces*, vol. 7, pp. 5134–5140, 2015.

[14] A. Hazra and P. Bhattacharyya, "Role of junction geometry in determining the rectification performance of nanostructures TiO_2-based p-n junctions," *IEEE Trans. Electron. Dev.*, vol. 62, no. 6, pp. 1984–1990, Jun. 2015.

[15] E. Hernandez-Rodriguez, A. Marquez-Herrera, E. Zaleta-Alejandre, M. Melendez-Lira, W. de la Cruz, and M. Zapata-Torres, "Effect of electrode type in the resistive switching behavior of TiO_2 thin films," *J. Phys. D, Appl. Phys.*, vol. 46, 2013, Art. no. 045103.

[16] N. Zhong, H. Shima, and H. Akinaga "Rectifying characteristic of Pt/TiO_x/metal/Pt controlled by electronegativity," *Appl. Phys. Lett.*, vol. 96, 2010, Art. no. 042107.

[17] W.-G. Kim and S.-W. Rhee, "Effect of the top electrode material on the resistive switching of TiO_2 thin film," *Microelectron. Eng.*, vol. 87, pp. 98–103, 2010.

[18] J. J. Yang *et al.*, "Metal/TiO_2 interfaces for memristive switches," *Appl. Phys. A*, vol. 102, pp. 785–789, 2011.

[19] S. C. Oh, H. Y. Jung, and H. Lee, "Effect of the top electrode materials on the resistive switching characteristics of TiO_2 thin films," *J. Appl. Phys.*, vol. 109, 2011, Art. no. 124511.

[20] P. Bousoulas, I. Michelakaki, and D. Tsoukalas, "Influence of Ti top electrode thickness on the resistive switching properties of forming free and self-rectified TiO_{2-x} thin films," *Thin Solid Films*, vol. 571, pp. 23–31, 2014.

[21] F. Hossein-Babaei, M. M. Lajvardi and N. Alaei-Sheini, "The energy barrier at noble metal/TiO_2 junctions," *Appl. Phys. Lett.*, vol. 106, 2015, Art. no. 083503.

[22] F. Hossein-Babaei, M. M. Lajvardi and N. Alaei-Sheini, "Oxygen adsorption at noble metal/TiO_2 junctions," in *Proc. IOP Conf. Ser. Mater. Sci. Eng.*, 2016, vol. 108, Art. no. 012030.

[23] S. M. Sze and K. K. Ng, *Physics of Semiconductor Devices*. Hoboken, NJ, USA: Wiley, 2006.

[24] R. Berdan, A. Serb, A. Khiat, A. Regoutz, C. Papavassilliou, and T. Prodromakis, "A μ-controller based system for interfacing selectorless RRAM crossbar arrays," *IEEE Trans. Electron. Dev.*, vol. 62, no. 7, pp. 2190–2196, Jul. 2015.

[25] D. Birmpiliotis, C. Czarneski, M. Koutsoureli, G. Papaioannou, and I. De Wolf, "Assessment of dielectric charging in capacitive MEMS switches fabricated on Si substrate with thin oxide film," *Microelectron. Eng.* vol. 159, pp. 209–214, 2016.

[26] Y. Wu, H. S. Gamble, B. M. Armstrong, V. F. Fusco, and J. A. Carson Stewart, "SiO_2 interface layer effects on microwave loss of high-resistivity CPW line," *IEEE Microw. Guided Wave Lett.* vol. 9, no. 1, pp. 10–12, Jan. 1999.

[27] C. E. Graves, N. Davila, E. J. Merced-Grafals, S.-T. Lam, J. P. Strachan, and R. S. Williams, "Temperature and field-dependent transport measurements in continuously tunable tantalum oxide memristors expose the dominant state variable," *Appl. Phys. Lett.*, vol. 110, 2017, Art. no. 123501.

[28] A. Mehonic *et al.*, "Intrinsic resistance switching in amorphous silicon oxide for high performance SiO_x ReRAM devices," *Microelectron. Eng.*, vol. 178, pp. 98–103, 2017.

[29] M. S. Munde *et al.*, "Intrinsic resistance switching in amorphous silicon suboxides: The role of columnar microstructure," *Sci. Rep.*, vol. 7, 2017, Art. no. 9274.

[30] S. Cortese, A. Khiat, D. Carta, M. E. Light, and T. Prodromakis, "An amorphous titanium dioxide metal insulator metal selector device for resistive random access memory crossbar array with tunable voltage margin," *Appl. Phys. Lett.*, vol. 108, 2016, Art. no. 033505.

[31] Y. Zhang *et al.*, "Vertically integrated ZnO-based 1D1R structure for resistive switching," *J. Phys. D, Appl. Phys.*, vol. 26, 2013, Art. no. 145101.

[32] Y. C. Shin *et al.*, "$(In,Sn)_2O_3/TiO_2$/Pt Schottky-type diode switch for the TiO_2 switching memory array," *Appl. Phys. Lett.*, vol. 92, 2008, Art. no. 162904.

[33] H. Choi, J. Shin, and C. Shin, "Impact of source/drain metal work function on the electrical characteristics of anatase TiO_2-based thin film transistors," *J. Solid State Sci. Technol.*, vol. 6, pp. P379–P382, 2017.

Authors' photographs and biographies not available at the time of publication.